

Report for ESRF Experiment 25-01-956 - XAS study of antiferromagnetic electrodeposited $\text{Fe}_x\text{Mn}_{1-x}$ thin films alloys

The results presented in this report has been published in S. Ruiz-Gómez et al. Phys. Chem. Chem. Phys. 18 (2016) 8212

Introduction

Nowadays, the possibility of producing cheap rare-earth-free iron-based permanent magnets is one of the most active topics in magnetic materials, with the goal to reduce the economic dependence on China. The coupling between ferromagnetic and antiferromagnetic iron based materials in the scale of nanometers can be used to produce magnetically hard materials taking advantage of the expected strong interfacial anisotropy [1,2]. Electrodeposition is a very suitable technique to grow structures with high-aspect ratio [3]. In these applications this is a key advantage because it allows exploiting also the shape anisotropy as an additional contribution to the total anisotropy in the magnet [4,5]. Therefore, the electrodeposition of an iron-based antiferromagnet is a promising step to address the challenge of creating rare-earth-free permanent magnets.

We have successfully electrodeposited $\text{Fe}_x\text{Mn}_{1-x}$ alloys for the first time and studied the magnetic properties of the obtained layers as a function of the Fe/Mn rate showing the possibility to electrodeposit antiferromagnetic FeMn alloys. The results, including the measurements carried out in this experiment, have been reported in Ref. 6.

Experimental

$\text{Fe}_x\text{Mn}_{1-x}$ films have been grown by electrochemical deposition from chloride-based electrolytes using Si/Ta/Au as a substrates. To avoid the formation of oxides in the electrolyte, the electrolyte was deaerated before electrodeposition using N_2 . Electrodeposition was carried out at room temperature, under stirring, in a three-electrode configuration, using Pt gauze as a counter electrode and an Ag/AgCl reference electrode.

The morphology and structure of the $\text{Fe}_x\text{Mn}_{1-x}$ films have been studied using different techniques (scanning electron microscopy, energy dispersive spectroscopy and x-ray diffraction). X-ray absorption experiments were performed on the SpLine beamline at the European Synchrotron Radiation Facility (ESRF). We carried out X-ray absorption near edge structure (XANES) spectroscopy experiments at the Fe K-edge (7.11 keV) and Mn K-edge (6.539 keV) in fluorescence mode at room temperature. Magnetic characterization has been carried out in VSM and SQUID magnetometers.

Results

We have electrodeposited for the first time $\text{Fe}_x\text{Mn}_{1-x}$ alloys and studied their magnetic properties as a function of the Fe/Mn rate. Figure 1.a shows typical FC-ZFC curves for Mn-rich samples. A phase transition can be shown at the Neel temperature of pure Mn. The hysteresis loop (Figure 1.b) has a ferromagnetic component and presents exchange bias. These curves can be explained considering that the films are composed of segregated Fe and Mn clusters.

Samples with composition close to $\text{Fe}_{50}\text{Mn}_{50}$ behave completely different. In particular, there is no transition in the FC-ZFC below 300 K (see figure 1.c). Considering that all $\text{Fe}_x\text{Mn}_{1-x}$ alloys are antiferromagnetic, this suggests that the Neel temperature is shifted to

temperatures above room temperature. In fact, a transition at 450 K is observed measuring the thermal evolution of magnetization above room temperature under an applied field of

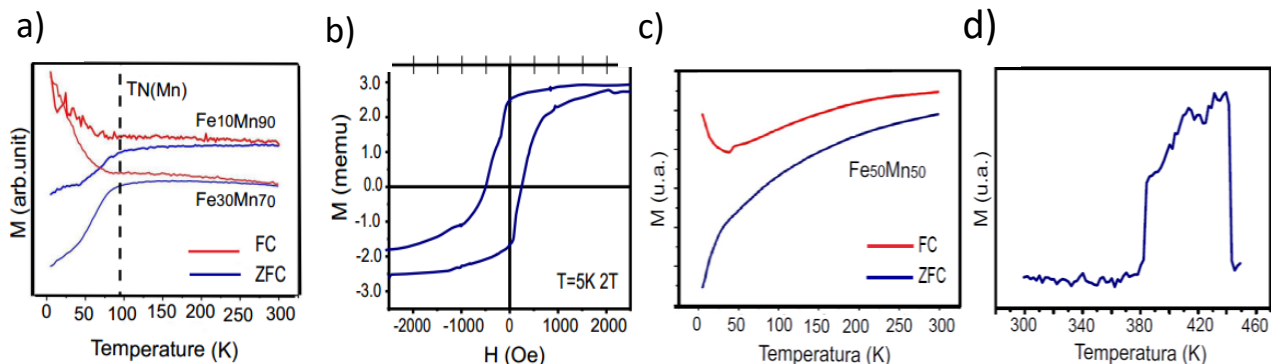


Fig. 1 (a) Thermal evolution of magnetization (FC–ZFC curves) and (b) hysteresis loop for samples rich in manganese and iron. The Neel temperature of pure Mn is indicated in the figure as a dashed line. (c) Thermal evolution of magnetization (FC–ZFC curves) and (d) Thermal evolution of magnetization measured at high (300–460 K) temperatures for samples with composition Fe₅₀Mn₅₀.

5000 Oe (see Figure 1.d). This could indicate that, in this case, Fe and Mn form an alloy.

Although the magnetic measurements indicate that we have successfully obtained an alloy when the composition is close to Fe₅₀Mn₅₀, structural measurements are necessary to confirm it and get more insight into the structure. In particular, it is necessary to know the local environment of Mn and Fe atoms in the films to elucidate whether they are forming an alloy or nanoclusters of the individual metals. We have performed XAS measurements on three electrodeposited layers with composition Mn₅₀Fe₅₀, Mn₃₀Fe₇₀ and Mn₇₀Fe₃₀. We have also measured pure Fe and Mn foils as well as a Mn₅₀Fe₅₀ foil as a reference. Fig. 2 shows the results obtained in the XAS measurements in the ESRF beamtime.

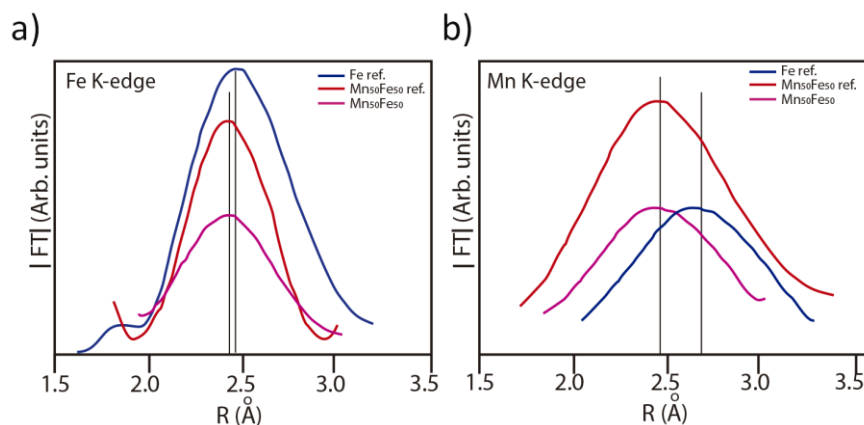


Fig. 2 (a) Fourier transform of the Fe K-edge and (b) Mn K-edge of the XANES signals measured in grown as well as reference samples. Red lines correspond to the fitting to a Lorentzian curve.

In fig. 2.a., we show the Fourier transform (FT) of the XANES data measured in the Fe K-edge. The comparison between the samples (Fe-rich, Mn-rich and Fe₅₀Mn₅₀) with the references provides us with information about the structure on the films. The position of the peaks for the different samples gives information about the bond length. As it can be seen in the figure, the position of the peak for the Fe-rich sample coincides with the position of the peak for the Fe reference foil, indicating that this sample it is not an alloy. Fe is segregated in the film forming clusters. In the Mn₅₀Fe₅₀ sample, the peak is shifted towards lower R

values, in the same way that it is shifted in the $Mn_{50}Fe_{50}$ reference foil. A similar behaviour is observed when measuring in the Mn K-edge (see Fig. 2b). The position of the peak for the Mn-rich sample coincides with the position of the peak for the Mn reference foil, showing the presence of segregated Mn clusters in the sample. Finally, in the case of the $Mn_{50}Fe_{50}$ electrodeposited sample, the peak position coincides with the one of the reference $Mn_{50}Fe_{50}$ foils. Thus, the analysis of the XANES data confirm the formation of an alloy in the case of the $Mn_{50}Fe_{50}$ electrodeposited films.

References

- [1] N. Jones, Nature 472 (2011) 22-23
- [2] C. Feng, B.H. Li, J. Teng, Y. Jiang and G.H. Yu. Thin Solid Films 517 (2009) 2745-2748
- [3] T. M. Whitney, P.C. Searson, J.S. Jiang and C.L. Chien, Science 231 (1993) 1316-1319
- [4] L. Sun, Y. Hao, C.L. Chien and P.C. Searson, IBM J. Res. Develop. 49 (2005) 79 - 102
- [5] B. Rodríguez-González et al., J. Appl. Phys. 115 (2014) 133904
- [6] S. Ruiz-Gomez et al, Phys. Chem. Chem. Phys. 18 (2016) 8212